

Metamagnetic transition in $\text{Ca}_{1-x}\text{Sr}_x\text{Co}_2\text{As}_2$ ($x = 0$ and 0.1) single crystals

J. J. Ying, Y. J. Yan, A. F. Wang, Z. J. Xiang, P. Cheng, G. J. Ye and X. H. Chen*
*Hefei National Laboratory for Physical Science at Microscale and Department of Physics,
University of Science and Technology of China, Hefei,
Anhui 230026, People's Republic of China*

We report the magnetism and transport measurements of CaCo_2As_2 and $\text{Ca}_{0.9}\text{Sr}_{0.1}\text{Co}_2\text{As}_2$ single crystals. Antiferromagnetic transition was observed at about 70 K and 90 K for CaCo_2As_2 and $\text{Ca}_{0.9}\text{Sr}_{0.1}\text{Co}_2\text{As}_2$, respectively. Magnetism and magnetoresistance measurements reveal metamagnetic transition from an antiferromagnetic state to a ferromagnetic state with the critical field of 3.5 T and 1.5 T respectively along c -axis for these two materials at low temperature. For the field along ab -plane, spins can also be fully polarized above the field of 4.5 T for $\text{Ca}_{0.9}\text{Sr}_{0.1}\text{Co}_2\text{As}_2$. While for CaCo_2As_2 , spins can not be fully polarized up to 7 T. We proposed the cobalt moments of these two materials should be ordered ferromagnetically within the ab -plane but antiferromagnetically along the c -axis (A-type AFM).

PACS numbers: 74.25.-q, 74.25.Ha, 75.30.-m

I. INTRODUCTION

The layered ThCr_2Si_2 structure type is commonly observed for AT_2X_2 compounds, in which A is typically a rare earth, alkaline earth, or alkali element; T is a transition-metal and X is metalloid element. In this ThCr_2Si_2 structure, the T_2X_2 layers are made from edge-sharing TX_4 tetrahedra and A ions are intercalated between T_2X_2 layers. Novel physical properties were observed in such ThCr_2Si_2 structure compounds including magnetic ordering and superconductivity. Recent discoveries of high temperature superconductivity in ThCr_2Si_2 structure pnictides and selenides have led to renewed interest in this large class of compounds^{1,2}. AFe_2As_2 ($A=\text{Ca}, \text{Sr}, \text{Ba}, \text{Eu}$) with the ThCr_2Si_2 -type structure were widely investigated because it is easy to grow large-size, high-quality single crystals^{3,4}. Superconductivity can be achieved through doping or under high pressure. The maximum T_c for the hole-doped samples is about 38 K and for the Co doped samples the maximum T_c can reach 26 K^{1,5}. Superconductivity up to 30 K was observed in $A_x\text{Fe}_{2-y}\text{Se}_2$ ($A=\text{K}, \text{Rb}, \text{Cs}$ and Tl) which also has the ThCr_2Si_2 structure^{2,6-10}. It is very interesting to look for other materials with related structures and investigate their physical properties to see if there can be potential parent compounds for new high temperature superconductors.

ACo_2As_2 (A is rare earth element) has the ThCr_2Si_2 structure, while their physical properties haven't been systematically studied. The magnetic moment of the Co ion in this type of material would not vanish due to the odd number of 3d electron, thus we would anticipate an appearance of the magnetic ordering phase. The magnetic properties of SrCo_2As_2 show Curie-Weiss-like behavior and BaCo_2As_2 was reported as a highly

renormalized paramagnet in proximity to ferromagnetic character^{11,12}. LaOCoAs with the same CoAs layers shows itinerant ferromagnetism¹³. While CaCo_2P_2 was reported as having ferromagnetically ordered Co planes, which are stacked antiferromagnetically²¹. The magnetic phase diagram of $\text{Sr}_{1-x}\text{Ca}_x\text{Co}_2\text{P}_2$ is very complicated and closely related to the structural changes¹⁸. The magnetism behavior in CoAs layered compounds is very interesting and it needs further investigation.

In this article, we investigated the magnetism and transport properties of CaCo_2As_2 and $\text{Ca}_{0.9}\text{Sr}_{0.1}\text{Co}_2\text{As}_2$ single crystals. Antiferromagnetic (AFM) ordering was observed below $T_N \approx 70$ K in CaCo_2As_2 . And for $\text{Ca}_{0.9}\text{Sr}_{0.1}\text{Co}_2\text{As}_2$, T_N increases to about 90 K. We determined the cobalt moments should be ordered ferromagnetically within the ab -plane but antiferromagnetically along the c -axis (A-type AFM). Metamagnetic transition corresponds to a spin-flop transition from an AF to a FM state was observed in these two samples.

II. EXPERIMENTAL DETAILS

High quality single crystals with nominal composition $\text{Ca}_{1-x}\text{Sr}_x\text{Co}_2\text{As}_2$ ($x=0$ and 0.1) were grown by conventional solid-state reaction using CoAs as self-flux¹¹. The CoAs precursor was first synthesized from stoichiometric amounts of Co and As inside the silica tube at 700 °C for 24 h. Then, the mixture with ratio of $\text{Ca}:\text{Sr}:\text{CoAs}=1-x:x:4$ was placed in an alumina crucible, and sealed in a quartz tube. The mixture was heated to 1200 °C in 6 hours and then kept at this temperature for 10 hours, and later slowly cooled down to 950 °C at a rate of 3 °C/hour. After that, the temperature was cooled down to room temperature by shutting down the furnace. The shining platelike $\text{Ca}_{1-x}\text{Sr}_x\text{Co}_2\text{As}_2$ crystals were mechanically cleaved. The actual composition of the single crystals were characterized by the Energy-dispersive X-ray spectroscopy (EDX). The actual doping levels are almost

*Corresponding author; Electronic address: chenxh@ustc.edu.cn

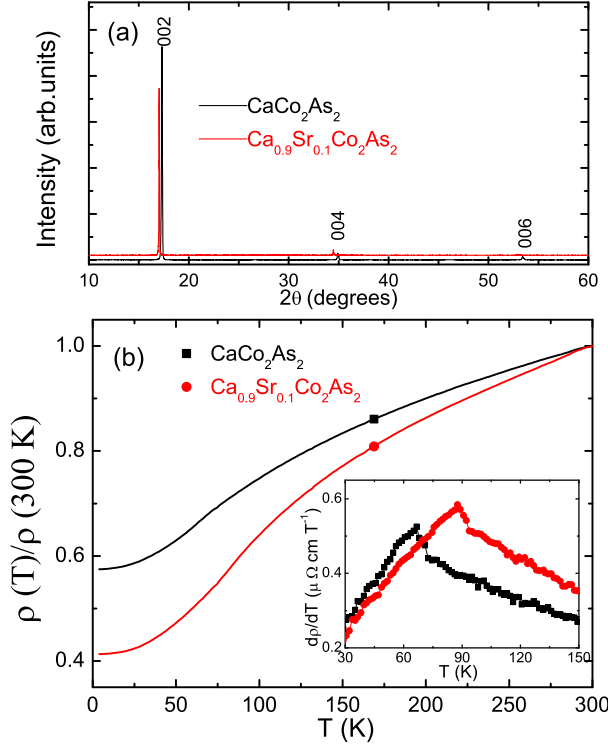


FIG. 1: (color online). (a): The single crystal x-ray diffraction pattern of CaCo_2As_2 and $\text{Ca}_{0.9}\text{Sr}_{0.1}\text{Co}_2\text{As}_2$. (b): Temperature dependence of in-plane resistivity for CaCo_2As_2 and $\text{Ca}_{0.9}\text{Sr}_{0.1}\text{Co}_2\text{As}_2$ single crystals. The inset was the derivation of resistivity curves around T_N .

the same as the nominal values. Resistivity was measured using the Quantum Design PPMS-9 and Magnetic susceptibility was measured using the Quantum Design SQUID-VSM.

III. RESULTS AND DISCUSSION

A. Crystal structure and resistivity

Single crystals of $\text{Ca}_{1-x}\text{Sr}_x\text{Co}_2\text{As}_2$ ($x = 0$ and 0.1) were characterized by X-ray diffractions (XRD) using $\text{Cu } K_\alpha$ radiations as shown in Fig.1(a). Only $(00l)$ diffraction peaks were observed, suggesting uniform crystallographic orientation with the c axis perpendicular to the plane of the single crystal. The c -axis parameter was about 10.27 \AA for CaCo_2As_2 which is nearly the same as the previous result¹⁹. For $\text{Ca}_{0.9}\text{Sr}_{0.1}\text{Co}_2\text{As}_2$, c -axis parameter increases to 10.41 \AA due to the larger ion radius of Sr. The resistivity of both samples shows metallic behavior as shown in Fig.1(b) which is similar to SrCo_2As_2 and BaCo_2As_2 ^{5,12}. The derivation of resistivity curves as shown in the inset of Fig.1(b) show peaks at about 70 and 90 K for CaCo_2As_2 and $\text{Ca}_{0.9}\text{Sr}_{0.1}\text{Co}_2\text{As}_2$, respectively. These temperatures were consistent with the antiferro-

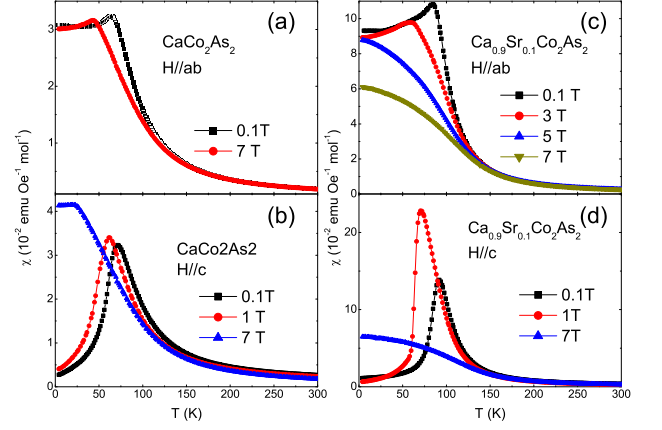


FIG. 2: (color online). Temperature dependence of the susceptibility for CaCo_2As_2 with magnetic field along (a) and perpendicular (b) to the ab -plane. Temperature dependence of the susceptibility for $\text{Ca}_{0.9}\text{Sr}_{0.1}\text{Co}_2\text{As}_2$ with magnetic field along (c) and perpendicular (d) to the ab -plane.

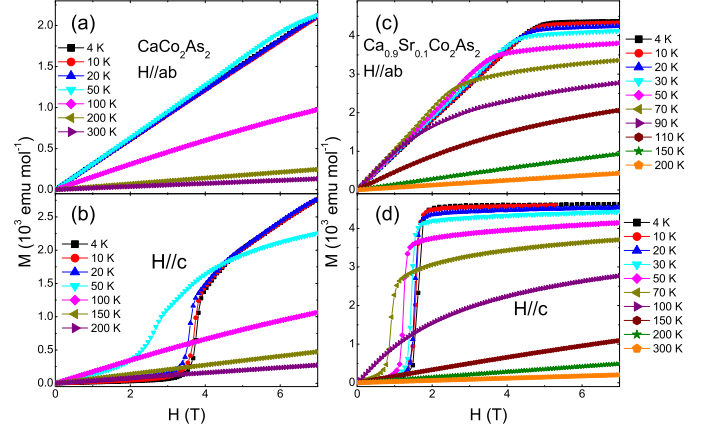


FIG. 3: (color online). Isothermal magnetization hysteresis of CaCo_2As_2 with magnetic field along (a) and perpendicular (b) to the ab -plane. MH curves for $\text{Ca}_{0.9}\text{Sr}_{0.1}\text{Co}_2\text{As}_2$ with field along (c) and perpendicular (d) to the ab -plane at certain temperature.

magnetic transition temperature (T_N) which would be shown later in the magnetic susceptibility measurements.

B. Magnetic susceptibility and magnetoresistance

Figure 2 (a) and (b) show the temperature dependence of susceptibility for CaCo_2As_2 under various magnetic field up to 7 T applied within ab -plane and along c -axis, respectively. The susceptibility drops at around 70 K with the field of 0.1 T applied along and perpendicular to the ab -plane, which indicates the antiferromagnetic state below 70 K in this material. T_N was suppressed by

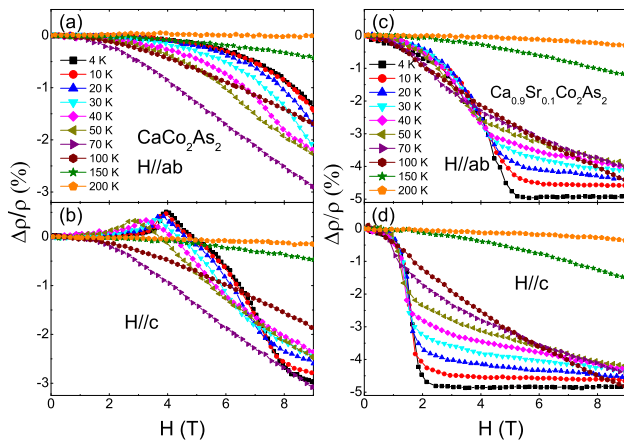


FIG. 4: (color online). Magnetoresistance of CaCo_2As_2 with magnetic field up to 9T along (a) and perpendicular (b) to the ab-plane. MR curves for $\text{Ca}_{0.9}\text{Sr}_{0.1}\text{Co}_2\text{As}_2$ with field along (c) and perpendicular (d) to the ab-plane at certain temperature.

increasing the field and was suppressed to 50 K under the field of 7 T applied along the ab-plane. However, with the field of 7 T applied along the c-axis, the susceptibility saturated at low temperature which indicated the ferromagnetic state at low temperature. For $\text{Ca}_{0.9}\text{Sr}_{0.1}\text{Co}_2\text{As}_2$, T_N increases to 90 K. Under high magnetic field, the system changes to ferromagnetic state with field applied both along and perpendicular to the ab-plane as shown in Fig. 2 (c) and (d). These results indicate that a metamagnetic transition from antiferromagnetism (AFM) to ferromagnetism (FM) occurs with increasing magnetic field at low temperature.

In order to further investigate such metamagnetic transition, we performed the isothermal magnetization hysteresis measurement as shown in Figure 3. The magnetization (M) almost increases linearly for CaCo_2As_2 with the field H applied along the ab-plane at various temperatures. The slope of MH curves is almost the same below 50 K and decrease with increasing the temperature above T_N . While for the field applied along the c-axis, M increases very sharply when H increases to about 3.5 T at 4 K. With increasing the temperature, such behavior weakened and vanished above T_N . This behavior clearly indicates the spin reorientation in CaCo_2As_2 at high magnetic field. While for $\text{Ca}_{0.9}\text{Sr}_{0.1}\text{Co}_2\text{As}_2$, M increases very steeply with H increasing to 1.5 T and saturates at high field with the field applied along the c-axis at 4 K. The transition field gradually decreases with increasing the temperature and vanishes above T_N . M increases almost linearly with H applied along ab-plane at low field at 4 K which is similar to the CaCo_2As_2 , further increasing the field leads to the saturation of M. The values of the saturated M are almost the same for the field along and perpendicular to the ab-plane. This result clearly indicates that almost all the magnetic ions can be tuned by the magnetic field above a critical field.

The critical magnetic field of $\text{Ca}_{0.9}\text{Sr}_{0.1}\text{Co}_2\text{As}_2$ is lower than CaCo_2As_2 , which is probably due to the weakening of inter layer AFM coupling. Spins can be tuned much easier with magnetic field applied along c-axis than along ab-plane, for CaCo_2As_2 , spins could not be aligned along ab-plane even under 7 T.

We further measured the magnetoresistance (MR) of CaCo_2As_2 and $\text{Ca}_{0.9}\text{Sr}_{0.1}\text{Co}_2\text{As}_2$ from 4 to 200 K up to 9 T as shown in Figure 4. Magnetoresistance can be hardly detected at high temperature and gradually became negative with decreasing the temperature. For CaCo_2As_2 , the magnitude of magnetoresistance gradually increases above T_N and gradually decreases below T_N with decreasing the temperature. This is because the presence of the FM order tends to suppress the spin scattering. Magnetic field gradually polarized the spins of Co ions with decreasing the temperature above T_N , while below the AFM transition temperature, it became much more difficult to polarize the spins with the temperature cooling down. The MR with H perpendicular to the ab-plane was almost the same with H along ab-plane above T_N . While the temperature below T_N , MR became positive at low magnetic field. When the applied magnetic field surpass the critical field of metamagnetic transition, MR gradually becomes negative and its magnitude increases with increasing the magnetic field. Similar MR behavior was observed above T_N with field applied along and perpendicular to the ab-plane. The MR changes greatly at the critical field of metamagnetic transition. The metamagnetic transition of $\text{Ca}_{0.9}\text{Sr}_{0.1}\text{Co}_2\text{As}_2$ is much sharper comparing with CaCo_2As_2 with H applied along c-axis. MR became constant when all the spins were tuned to FM state. The values of MR are almost the same for the field along and perpendicular to the ab-plane which indicates that all the spins can be tuned by high magnetic field. Similar MR behaviors across the AF and the FM phase boundary were also observed in other materials such as $\text{Na}_{0.85}\text{CoO}_2$, layered ruthenates and colossal magnetoresistance materials^{14,15}. The MR result about the metamagnetic transition is consistent with the MH measurements in these two materials. The magnetoresistance with field applied along and perpendicular to the ab-plane are almost the same under high magnetic field which indicates that magnetoresistance was mainly induced from magnetic scattering from Co^{2+} and all the Co^{2+} spins can be tuned above the critical field of metamagnetic transition at low temperature.

C. Hall coefficient and magnetic structure

We also measured the Hall resistivity ρ_{xy} of CaCo_2As_2 and $\text{Ca}_{0.9}\text{Sr}_{0.1}\text{Co}_2\text{As}_2$ as shown in Figure 5. ρ_{xy} is measured by sweeping field from -7 T to +7 T at various temperature, thus the accurate Hall resistivity ρ_H is obtained by using $[\rho_{xy}(+H) - \rho_{xy}(-H)]/2$, where $\rho_{xy}(\pm H)$ is ρ_{xy} under positive or negative magnetic field. We found ρ_{xy} shows a steep decrease at certain field H_C below T_N

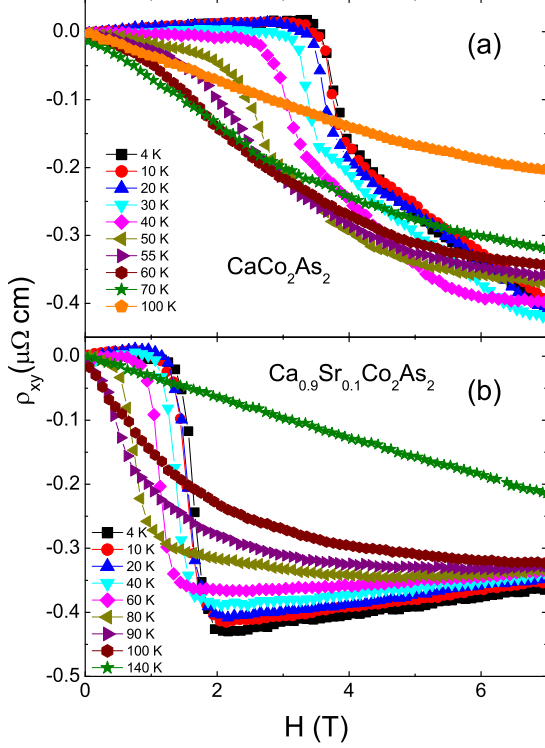


FIG. 5: (color online). Field dependence of Hall resistivity at various temperatures for CaCo_2As_2 (a) and $\text{Ca}_{0.9}\text{Sr}_{0.1}\text{Co}_2\text{As}_2$ (b).

similar to isothermal MR, which arises from the jump magnitudes of magnetization \mathbf{M} due to the spin-flop of Co ions induced by external field \mathbf{H} . It is well known that Hall effect arises from two parts of normal Hall effect and anomalous Hall effect in ferromagnetic metals, in which anomalous Hall resistivity is proportional to the magnetization \mathbf{M} . Hall resistivity $\rho_{xy} = R_H^N H + R_H^A 4\pi M$, where R_H^N is the normal Hall coefficient, and R_H^A is the anomalous Hall coefficient¹⁶. We extracted the R_H^N from H-linear term of ρ_{xy} at low field. Temperature dependence of R_H^N for CaCo_2As_2 and $\text{Ca}_{0.9}\text{Sr}_{0.1}\text{Co}_2\text{As}_2$ are shown in Fig.6(a) and (b), respectively. The value of R_H^N is negative at high temperature, indicating the primary carrier in these two materials is electron. The magnitude of R_H^N gradually increases with decreasing the temperature and it reaches its maximum value at around T_N . Below T_N , the magnitude of R_H^N decreases very quickly with decreasing the temperature. The anomalous Hall coefficient R_H^A below T_N is inferred from the ratio of the jump magnitudes ΔM and $\Delta\rho_{xy}$ around metamagnetic transition field. $R_H^A = \Delta\rho_{xy}/4\pi\Delta M$ is also plotted in Fig.6 (a) and (b). The magnitude of R_H^A decreases linearly with decreasing temperature below T_N . Such behavior was also observed in $\text{TaFe}_{1+y}\text{Te}_3$ system¹⁷.

Based on the above results of magnetic susceptibility,

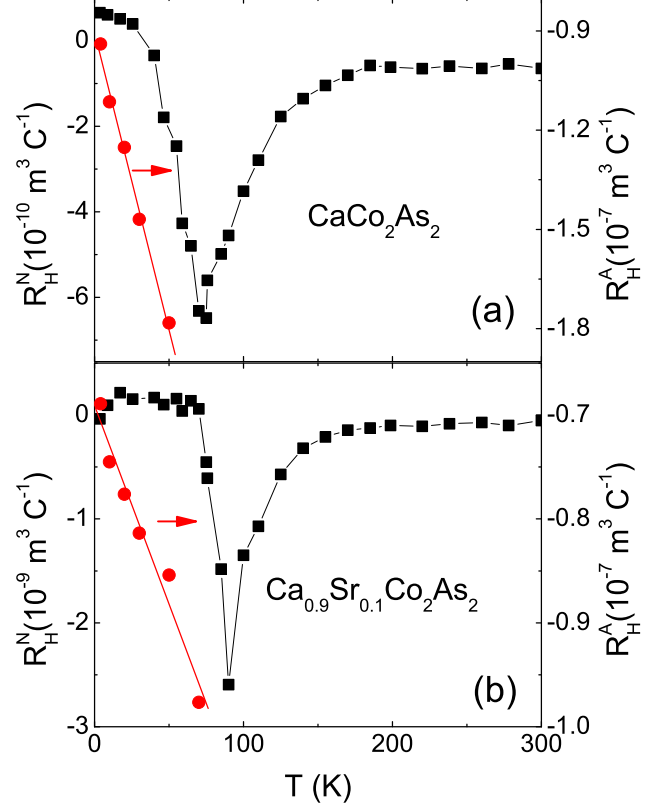


FIG. 6: (color online). The temperature dependence of anomalous Hall coefficient R_H^A and normal Hall coefficient R_H^N for CaCo_2As_2 (a) and $\text{Ca}_{0.9}\text{Sr}_{0.1}\text{Co}_2\text{As}_2$ (b).

MR and Hall resistivity measurement, possible magnetic structures for the spins of Co ions are proposed as shown in Fig. 7 (a), (b) and (c). Below T_N , Co spins of these two materials should be ordered ferromagnetically within the ab-plane but antiferromagnetically along the c-axis (A-type AFM) under low magnetic field. When the external field surpasses the inner field H_{int} of Co spins. All the Co spins aligned along the direction of \mathbf{H} . The external field \mathbf{H} along ab-plane is much harder to tune the AFM ordering of Co spins than with \mathbf{H} along c-axis.

The AFM ordering found in CaCo_2As_2 and $\text{Ca}_{0.9}\text{Sr}_{0.1}\text{Co}_2\text{As}_2$ is very different from their isostructure compounds SrCo_2As_2 and BaCo_2As_2 in which no magnetic ordering was observed. Such a difference might due to the much smaller c/a ratio in CaCo_2As_2 than in SrCo_2As_2 and BaCo_2As_2 , similar properties were also observed in CaCo_2P_2 ¹⁸. High magnetic field can tune almost all the spins, and metamagnetic transition was observed by increasing the magnetic field at low temperature which was similar to EuFe_2As_2 ²⁰. The magnetic property in this system is strongly correlated to the structure. The critical field of metamagnetic

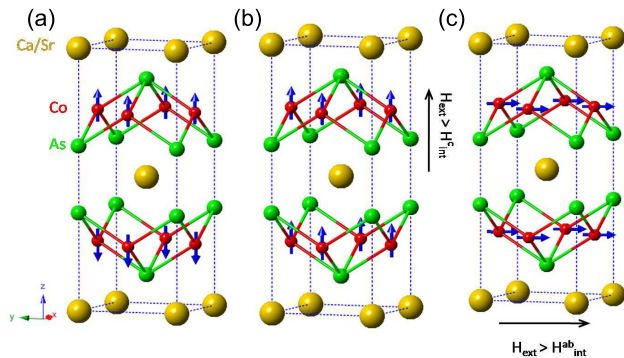


FIG. 7: (color online). (a): Possibly magnetic structure deduced from magnetism and MR measurement. Magnetic structure above the critical field with H along (b) and perpendicular (c) to c -axis.

transition decreased by doping Sr, which was probably due to the enlarged c -axis parameter and decreased the inter layer AFM coupling.

IV. CONCLUSION

In conclusion, we found AFM ordering in CaCo_2As_2 and $\text{Ca}_{0.9}\text{Sr}_{0.1}\text{Co}_2\text{As}_2$ at 70 and 90 K, respectively. A metamagnetic transition from AFM to FM occurs with increasing magnetic field in these two compounds. Little Sr doping in CaCo_2As_2 would effectively decrease the critical field of metamagnetic transition. The magnetic susceptibility and MR measurements all indicate that the cobalt moments of these two materials should be ordered ferromagnetically within the ab -plane but antiferromagnetically along the c -axis (A-type AFM), which is the same with their isostructure compound CaCo_2P_2 ^{21,22}.

ACKNOWLEDGEMENT This work is supported by the National Basic Research Program of China (973 Program, Grant No. 2012CB922002 and No. 2011CB00101), National Natural Science Foundation of China (Grant No. 11190021 and No. 51021091), the Ministry of Science and Technology of China, and Chinese Academy of Sciences.

- ¹ M. Rotter, M. Tegel, D. Johrendt, Phys. Rev. Lett. **101**, 107006(2008).
- ² J. Guo, S. Jin, G. Wang, S. Wang, K. Zhu, T. Zhou, M. He and X. Chen, Phys. Rev. B **82**, 180520(R) (2010).
- ³ G Wu, H Chen, TWu, Y L Xie, Y J Yan, R H Liu, X FWang, J J Ying and X H Chen, J. Phys.: Condens. Matter **20** 422201 (2008)
- ⁴ X. F. Wang, T. Wu, G. Wu, H. Chen, Y. L. Xie, J. J. Ying, Y. J. Yan, R. H. Liu and X. H. Chen, Phys. Rev. Lett. **102**, 117005(2009).
- ⁵ Athena S. Sefat, Rongying Jin, Michael A. McGuire, Brian C. Sales, David J. Singh, and David Mandrus, Phys. Rev. Lett. **101**, 117004 (2008).
- ⁶ Yoshikazu Mizuguchi, Hiroyuki Takeya, Yasuna Kawasaki, Toshinori Ozaki, Shunsuke Tsuda, Takahide Yamaguchi and Yoshihiko Takano, Appl. Phys. Lett. **98**, 042511 (2011).
- ⁷ A. F. Wang, J. J. Ying, Y. J. Yan, R. H. Liu, X. G. Luo, Z. Y. Li, X. F. Wang, M. Zhang, G. J. Ye, P. Cheng, Z. J. Xiang, X. H. Chen, Phys. Rev. B **83**, 060512(R) (2011).
- ⁸ J. J. Ying, X. F. Wang, X. G. Luo, A. F. Wang, M. Zhang, Y. J. Yan, Z. J. Xiang, R. H. Liu, P. Cheng, G. J. Ye, X. H. Chen, Phys. Rev. B **83**, 212502 (2011).
- ⁹ A. Krzton-Maziopa, Z. Shermadini, E. Pomjakushina, V. Pomjakushin, M. Bendele, A. Amato, R. Khasanov, H. Luetkens and K. Conder, J. Phys.: Condens. Matter **23**, 052203 (2011).
- ¹⁰ Minghu Fang, Hangdong Wang, Chiheng Dong, Zujuan Li, Chunmu Feng, Jian Chen, H.Q. Yuan, EPL, **94**, 27009 (2011).
- ¹¹ A. S. Sefat, D. J. Singh, R. Jin, M. A. McGuire, B. C. Sales, and D. Mandrus, Phys. Rev. B **79**, 024512 (2009).
- ¹² A. Leithe-Jasper, W. Schnelle, C. Geibel, and H. Rosner, Phys. Rev. Lett. **101**, 207004 (2008).
- ¹³ H. Yanagi, R. Kawamura, T. Kamiya, Y. Kamihara, M. Hirano, T. Nakamura, H. Osawa, and H. Hosono, Phys. Rev. B **77**, 224431 (2008).
- ¹⁴ J. L. Luo, N. L. Wang, G.T. Liu, D. Wu, X. N. Jing, F. Hu, and T. Xiang, Phys. Rev. Lett. **93**, 187203 (2004).
- ¹⁵ S. Nakatsuji, D. Hall, L. Balicas, Z. Fisk, K. Sugahara, M. Yoshioka, and Y. Maeno, Phys. Rev. Lett. **90**, 137202 (2003).
- ¹⁶ N. Nagaosa, J. Sinova, S. Onoda, A. H. MacDonald, and N. P. Ong, Rev. Mod. Phys. **82**, 1539(2010).
- ¹⁷ R. H. Liu, M. Zhang, P. Cheng, Y. J. Yan, Z. J. Xiang, J. J. Ying, X. F. Wang, A. F. Wang, G. J. Ye, X. G. Luo, and X. H. Chen, Phys. Rev. B **84**, 184432 (2011).
- ¹⁸ Shuang Jia, A. J. Williams, P. W. Stephens, and R. J. Cava, Phys. Rev. B **80**, 165107 (2009).
- ¹⁹ David C. Johnston, Advances in Physics **59**, 803C1061 (2010).
- ²⁰ T. Wu, G. Wu, H. Chen, Y. L. Xie, R. H. Liu, X. F. Wang and X. H. Chen, J. Mag. Mag. Mat. **321**, 3870-3874 (2009).
- ²¹ M. Reehuis and W. Jeitschko, J. Phys. Chem. Solids **51**, 961 (1990).
- ²² M. Reehuis, W. Jeitschko, G. Kotzyba, B. Zimmer, and X. Hu, J. Alloys Compd. **266**, 54 (1998).